

The puzzling origin of the ${}^6\text{Li}$ plateau

Carmelo Evoli,^{*} Stefania Salvadori and Andrea Ferrara

SISSA/International School for Advanced Studies, Via Beirut 4, 34100 Trieste, Italy

Accepted 2008 June 25. Received 2008 June 25; in original form 2008 May 17

ABSTRACT

We discuss the ${}^6\text{Li}$ abundance evolution within a hierarchical model of Galaxy formation which correctly reproduces the $[\text{Fe}/\text{H}]$ distribution of metal-poor halo stars. Contrary to previous findings, we find that neither the level (${}^6\text{Li}/\text{H} = 6 \times 10^{-12}$) nor the flatness of the ${}^6\text{Li}$ distribution with $[\text{Fe}/\text{H}]$ can be reproduced under the most favourable conditions by any model in which ${}^6\text{Li}$ production is tied to a (data-constrained) Galactic star formation rate via cosmic ray spallation. Thus, the origin of the plateau might be due to some other early mechanism unrelated to star formation.

Key words: nuclear reactions, nucleosynthesis, abundances – stars: abundances – stars: formation – cosmic rays – galaxies: evolution – cosmology: theory.

1 INTRODUCTION

The relative abundance of light elements synthesized during the big bang nucleosynthesis (BBN) is a function of a single parameter, η , namely the baryon-to-photon ratio. Given the *WMAP* constraint $\eta = (6.8 \pm 0.21) \times 10^{-10}$, the light nuclei abundances can be precisely predicted by BBN (Yao et al. 2006; Spergel et al. 2007). Despite a general agreement with the observed abundances of light elements, discrepancies arise concerning Li abundance. Observationally, the primordial abundance of lithium isotopes (${}^7\text{Li}$ and ${}^6\text{Li}$) is measured in the atmospheres of Galactic metal-poor halo stars (MPHS).

Since the first detection by Spite & Spite (1982), later confirmed by subsequent works (Spite, Spite & Maillard 1984; Ryan, Norris & Beers 1999; Asplund et al. 2006; Bonifacio et al. 2007), a ${}^7\text{Li}/\text{H} = (1\text{--}2) \times 10^{-10}$ abundance was deduced, independent of stellar $[\text{Fe}/\text{H}]$. The presence of such a ${}^7\text{Li}$ plateau supports the idea that ${}^7\text{Li}$ is a primary element, synthesized by BBN. The measured value, however, results of a factor of 2–4 lower than that the expected from the BBN ${}^7\text{Li}/\text{H} = 4.27_{-0.83}^{+1.02} \times 10^{-10}$ (Cyburt 2004), ${}^7\text{Li}/\text{H} = 4.9_{-1.2}^{+1.4} \times 10^{-10}$ (Cuoco et al. 2004) or ${}^7\text{Li}/\text{H} = 4.15_{-0.45}^{+0.49} \times 10^{-10}$ (Coc et al. 2004). Recently, Pinsonneault et al. (2002), Korn et al. (2006) found that mixing and diffusion processes during stellar evolution could reduce the ${}^7\text{Li}$ abundance in stellar atmospheres by about 0.2 dex, thus partially releasing the tension.

A more serious problem arose with ${}^6\text{Li}$, for which the BBN predicts a value of $({}^6\text{Li}/\text{H})_{\text{BBN}} \sim 10^{-14}$. Owing to the small difference in mass between ${}^6\text{Li}$ and ${}^7\text{Li}$, lines from these two isotopes blend easily. The detection of ${}^6\text{Li}$ then results quite difficult since the predominance of ${}^7\text{Li}$. Recently, high-resolution spectroscopic observations measured the ${}^6\text{Li}$ abundance in 24 MPHS (Asplund et al. 2006), revealing the presence of a plateau ${}^6\text{Li}/\text{H} = 6 \times 10^{-12}$ for $-3 \lesssim [\text{Fe}/\text{H}] \lesssim -1$. A primordial origin of ${}^6\text{Li}$ seems favoured by

the presence of the plateau; however, the high ${}^6\text{Li}$ value observed cannot be reconciled with this hypothesis.

The solutions invoked to overcome the problem were: (i) a modification of BBN models (Kawasaki, Kohri & Moroi 2005; Jedamzik et al. 2006; Pospelov 2007; Cumberbatch et al. 2007; Kusakabe et al. 2007), (ii) the fusion of ${}^3\text{He}$ accelerated by stellar flares with the atmospheric helium (Tatischeff & Thibaud 2007), (iii) a mechanism allowing for later production of ${}^6\text{Li}$ during Galaxy formation. The latter scenario involves the generation of cosmic rays (CRs). ${}^6\text{Li}$, in fact, can be synthesized by fusion reactions ($\alpha + \alpha \rightarrow {}^6\text{Li}$) when high-energy CR particles collide with the ambient gas. Energetic CRs can either be accelerated by shock waves produced during cosmological structure formation processes (Miniati et al. 2000; Suzuki & Inoue 2002; Keshet et al. 2003) or, by strong supernova (SN) shocks along the build-up of the Galaxy. In their recent work, Rollinde, Vangioni & Olive (2006) used the supernova rate (SNR) by Daigne et al. (2006) to compute the production of ${}^6\text{Li}$ in the intergalactic medium (IGM). Assuming that all MPHS form at $z \sim 3$, and from a gas with the same IGM composition, they obtained the observed ${}^6\text{Li}$ value. Despite the apparent success of the model, these assumptions are very idealized and require a closer inspection. We revisit the problem using a more realistic and data-constrained approach, based on the recent model by Salvadori, Schneider & Ferrara (2007) (SSF07), which follows the hierarchical build-up of the Galaxy and reproduces the metallicity distribution of MPHS.

2 BUILDING THE MILKY WAY

The code GALaxy Merger Tree and Evolution (GAMETE) described in SSF07 (updated version in Salvadori, Ferrara & Schneider 2008) follows the star formation (SF)/chemical history of the MW along its merger tree, finally matching all its observed properties.

The code reconstructs the hierarchical merger history of the MW using a Monte Carlo algorithm based on the extended Press &

^{*}E-mail: evoli@sissa.it

Schechter theory (Press & Schechter 1974) and adopting a binary scheme with accretion mass (Cole et al. 2000; Volonteri, Haardt & Madau 2003). Looking back in time at any time-step, a halo can either lose part of its mass (corresponding to a cumulative fragmentation into haloes below the resolution limit M_{res}) or lose mass and fragment into two progenitors. The mass below M_{res} accounts for the *Galactic Medium* (GM) which represents the mass reservoir into which haloes are embedded. During the evolution, progenitor haloes accrete gas from the GM and virialize out of it. We assume that feedback suppresses SF in mini-haloes and that only Ly α cooling haloes ($T_{\text{vir}} > 10^4\text{K}$) contribute stars and metals to the Galaxy. This motivates the choice of a resolution mass $M_{\text{res}} = M_4(z)/10 = M(T_{\text{vir}} = 10^4\text{K}, z)/10$ where $M_4(z)$ is the mass corresponding to a virial temperature $T_{\text{vir}} = 10^4\text{K}$ at redshift z . At the highest redshift of the simulation, $z \approx 20$, the gas present in virialized haloes, as in the GM, is assumed to be of primordial composition. The SF rate (SFR) is taken to be proportional to the mass of gas. Following the critical metallicity scenario (Bromm et al. 2001; Schneider et al. 2002, 2003; Omukai et al. 2005; Schneider et al. 2006), we assume that low-mass (Pop II/I) SF occurs when the metallicity $Z_{\text{cr}} > 10^{-5\pm 1} Z_{\odot}$ according to a Larson initial mass function with a characteristic mass $m_{\star} = 0.35 M_{\odot}$. At lower Z , massive Pop III stars form with a characteristic mass $m_{\text{Pop III}} = 200 M_{\odot}$, i.e. within the pair-instability supernova (SN_{PISN}) mass range of 140–260 M_{\odot} (Heger & Woosley 2002). The chemical evolution of both gas in protogalactic haloes (ISM) and in the GM, is computed by according to a mechanical feedback prescription (see Salvadori et al. 2008, for details). Produced metals are instantaneously and homogeneously mixed with the gas.

The model free parameters are fixed to match the global properties of the MW and the Metallicity Distribution Function (MDF) of MPHS derived from the Hamburg–European Southern Observatory (ESO) Survey (Beers & Christlieb, private communication). In Fig. 1 (upper panel), the derived Galactic (comoving) SFR density is shown for Pop III and Pop II/I stars. Pop II/I stars dominate the SFR at any redshift. Following a burst of Pop III stars, in fact, the metallicity of the host halo raises to $Z > Z_{\text{cr}}$: chemical feedback suppresses Pop III formation in self-enriched progenitors. Later on Pop III, stars can only form in those haloes which virialize from the GM and so, when $Z_{\text{GM}} \gtrsim Z_{\text{cr}}$, their formation is totally quenched. The above results are in agreement with recent hydrodynamic simulations implementing chemical feedback effects (Tornatore, Ferrara & Schneider 2007). The earlier Pop III disappearance of our model ($z \sim 10$) with respect to this study ($z \sim 4$) is a consequence of the biased volume we consider i.e. the MW environment. As the higher mean density accelerates SF/metal enrichment, Pop III stars disappear at earlier times; the SFR maximum value and shape, however, match closely the simulated ones.

In Fig. 1 (lower panel), we show the corresponding evolution of the GM iron and oxygen abundance. As SSF07 have shown that the majority of present-day iron-poor stars ($[\text{Fe}/\text{H}] < -2.5$) formed in haloes accreting GM gas which was Fe enhanced by the previous SN explosions, the initial $[\text{Fe}/\text{H}]$ abundance within a halo is set by the corresponding GM Fe-abundance at the virialization redshift.

3 LITHIUM PRODUCTION

To describe the production of ${}^6\text{Li}$ for a continuous source of CRs, we generalize the classical work of Montmerle (1977), who developed a formalism to follow the propagation of an homogeneous CR population in an expanding universe, assuming that CRs have been instantaneously produced at some redshift.

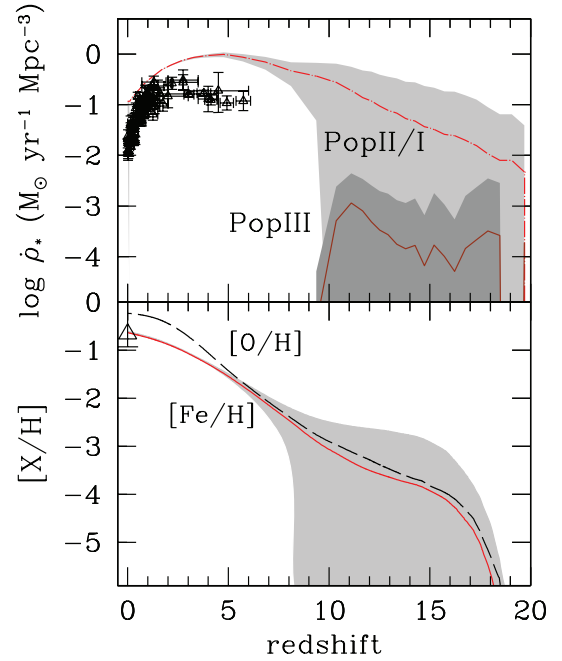


Figure 1. Upper panel: comoving SFR density evolution for Pop III (solid line) and Pop II/I stars (dashed line). The curves are obtained after averaging over 100 realizations of the merger tree; shaded areas denote $\pm 1\sigma$ dispersion regions around the mean. Points represent the low-redshift measurements of the cosmic SFR by Hopkins (2004). Lower panel: corresponding GM iron (solid line) and oxygen (dashed line) abundance evolution. The point is the measured $[\text{O}/\text{H}]$ abundance in high-velocity clouds by Ganguly et al. (2005).

Since the *primary* CRs are assumed to be produced by supernovae (SNe), the physical source function $Q(E, z)$ is described by a power law in momentum:

$$Q(E, z) = C(z) \frac{\phi(E)}{\beta(E)} (\text{GeV}/\text{n})^{-1} \text{cm}^{-3} \text{s}^{-1} \quad (1)$$

with $\beta = v/c$ and

$$\phi(E) = \frac{E + E_0}{[E(E + 2E_0)]^{(\gamma+1)/2}} (\text{GeV}/\text{n})^{-1} \text{cm}^{-2} \text{s}^{-1}, \quad (2)$$

where γ is the injection spectral index and $E_0 = 939\text{MeV}$ and E are, respectively, the rest-mass energy and the kinetic energy per nucleon. The functional form of the injection spectrum $\phi(E)$ is inferred from the theory of collisionless shock acceleration (Blandford & Eichler 1987) and the γ value is the one typically associated to the case of strong shock. We note, however, that the results are only very weakly dependent on the spectral slope. Finally, $C(z)$ is a redshift-dependent normalization; its value is fixed at each redshift by normalizing $Q(E, z)$ to the total kinetic energy transferred to CRs by SN explosions:

$$\mathcal{E}_{\text{SN}}(z) = \int_{E_{\text{min}}}^{E_{\text{max}}} E Q(E, z) dE \quad (3)$$

with

$$\mathcal{E}_{\text{SN}}(z) = \epsilon(1+z)^3 [E_{\text{II}} \text{SNR}_{\text{II}}(z) + E_{\gamma\gamma} \text{SNR}_{\gamma\gamma}(z)], \quad (4)$$

where $E_{\text{II}} = 1.2 \times 10^{51}$ and $E_{\gamma\gamma} = 2.7 \times 10^{52}$ erg are, respectively, the average explosion energies for a Type II SN (SN_{II}) and a $\text{SN}_{\gamma\gamma}$; $\epsilon = 0.15$ is the fraction of the total energy not emitted in neutrinos transferred to CRs by a single SN, assumed to be the same for the two stellar populations; SNR_{II} ($\text{SNR}_{\gamma\gamma}$) is the SN_{II} ($\text{SN}_{\gamma\gamma}$) explosion

comoving rate, simply proportional to the Pop III/I (Pop III) SFR. The efficiency parameter is inferred by shock acceleration theory and confirmed by recent observations of SN remnants in our Galaxy (Tatischeff 2008).

We now need to specify the energy limits E_{\min}, E_{\max} of the CR spectrum produced by SN shock waves (equation 3). We fix $E_{\max} = 10^6$ GeV, following the theoretical estimate by Lagage & Cesarsky (1983). Due to the rapid decrease in $\phi(E)$, the choice of E_{\max} does not affect the result of the integration and hence the derived $C(z)$ value. On the contrary, $C(z)$ strongly depends on the choice of E_{\min} : the higher E_{\min} , the higher is $C(z)$. Since observations cannot set tight constraints on E_{\min} , due to solar magnetosphere modulation of low- E CRs, we consider it as a free parameter of the model.

Once the spectral shape of $Q(E, z)$ is fixed, we should, in principle, take in account the subsequent propagation of CRs both in the ISM and GM. Following Rollinde et al. (2006), we make the hypothesis that primary CRs escape from parent galaxies on a time-scale short enough to be considered as immediately injected in the GM without energy losses. At high redshift in fact: (i) structures are smaller and less dense (Zhao et al. 2003) implying higher diffusion efficiencies (Jubelgas et al. 2006); (ii) the magnetic field is weaker and so it can hardly confine CRs into structures. Note also that, besides diffusive propagation of CRs, superbubbles and/or galactic winds could directly eject CRs into the GM.

Under this hypothesis, the density evolution of primary CRs only depends on energy losses suffered in the GM. The nuclei lose energy mainly via two processes, ionization and Hubble expansion, and they are destroyed by inelastic scattering of GM targets (mainly protons).

We can follow the evolution of α -particles (primary CRs) through the transport equation (Montmerle 1977)

$$\frac{\partial N_{\alpha,H}}{\partial t} + \frac{\partial}{\partial E}(bN_{\alpha,H}) + \frac{N_{\alpha,H}}{T_D} = K_{\alpha p} Q_{\alpha}(E, z), \quad (5)$$

where $N_{i,H}$ is the ratio between the (physical) number density of species i and GM protons, $n_H(z) = n_{H,0}(1+z)^3$; $Q_H(E, z) \equiv Q(E, z)/n_H(z)$ is the normalized physical source function, $b \equiv (\partial E/\partial t)$ is the total energy-loss rate adopted from Rollinde et al. (2006), T_D is the destruction term as in the analytic fit by Heinbach & Simon (1995); finally, $K_{\alpha p} = 0.08$ is the cosmological abundance by number of α -particles with respect to protons.

We consider ${}^6\text{Li}$ as entirely secondary, i.e. purely produced by fusion of GM He-nuclei by primary α -particles. The physical source function for ${}^6\text{Li}$ is given by

$$Q_{{}^6\text{Li}}(E, z) = \int \sigma_{\alpha\alpha\rightarrow{}^6\text{Li}}(E, E') n_{\text{He}}(z) \Phi_{\alpha}(E', z) dE', \quad (6)$$

where E' and E are, respectively, the kinetic energies per nucleon of the incident particle and of the produced ${}^6\text{Li}$ nuclei, and $\Phi_{\alpha}(E', z) = \beta(E') N_{\alpha}(E', z)$ the incident α -particle flux. Making the approximation $\sigma_{\alpha\alpha\rightarrow{}^6\text{Li}}(E, E') = \sigma_l(E) \delta(E - E'/4)$ (Meneguzzi, Audouze & Reeves 1971) and defining $Q_{{}^6\text{Li},H} \equiv Q_{{}^6\text{Li}}/n_H$, the equation (6) becomes

$$Q_{{}^6\text{Li},H}(E, z) = \sigma_l(E) K_{\alpha p} n_H(z) \Phi_{\alpha,H}(4E, z), \quad (7)$$

where the cross-section $\sigma_l(E)$ is given by the analytic fit of Mercer et al. (2001):

$$\sigma_l(E) \sim 66 \exp\left(-\frac{E}{4 \text{ MeV}}\right) \text{ mb}. \quad (8)$$

We can now write a very simple equation describing the evolution of ${}^6\text{Li}$:

$$\frac{\partial N_{{}^6\text{Li},H}}{\partial t} = Q_{{}^6\text{Li},H}(E, z) \quad (9)$$

in this case, in fact, destruction and energy losses are negligible since their time-scales are very long with respect to the production time-scale (Rollinde, Vangioni & Olive 2005).

The solution of the coupled equations (5)–(9) gives ${}^6\text{Li}/\text{H}$ at any given redshift z .

4 RESULTS

The system of equations introduced in the previous section is solved numerically using a Crank–Nicholson implicit numerical scheme (Press 2002). Because of its stability and robustness implicit schemes are used to solve transport equations in most CRs diffusion problems (Strong & Moskalenko 1998).

We test the accuracy of our code by studying a simplified case in which an analytic solution can be derived and compared with numerical results. To this aim, we assume that (i) both energy losses and destruction of primary CRs in the GM can be neglected; (ii) the physical energy density injected by SNe is constant, $\mathcal{E}_{\text{SN}} \sim 7.4 \times 10^{-27}$ GeV cm $^{-3}$ s $^{-1}$, in the redshift range $z > 3$. It is worth noting that the above hypothesis conspire to give an upper limit to the exact solution, thus providing an estimate of the maximum achievable ${}^6\text{Li}$ abundance. Under these approximations, the source spectrum defined in equation (1) becomes

$$Q(E, z) = 6.4 \cdot 10^{-29} \frac{\phi(E)}{\beta(E)} (\text{GeV/n})^{-1} \text{ cm}^{-3} \text{ s}^{-1} \quad (10)$$

and equations (5)–(9) can be solved. We find

$$N_{\alpha,H}(z) = 39.6 (1+z)^{-9/2} \quad (11)$$

and

$$N_{{}^6\text{Li},H}(z) = 8.2 \times 10^{-11} (1+z)^{-3}. \quad (12)$$

From Fig. 2, we conclude that the analytical solution for the GM ${}^6\text{Li}$ abundance (equation 12) is perfectly matched by the numerical one. Also shown are the numerical solutions obtained by relaxing first the hypothesis (i) and then (i) + (ii). Not unexpectedly, the inclusion of energy losses and destruction term into equation (5) affects only slightly the result, as the typical time-scales of such processes are longer than the ${}^6\text{Li}$ production one.

A realistic injection energy, on the contrary, has a strong impact on the predicted shape and amplitude of the ${}^6\text{Li}$ evolution. In fact, the SFR, and consequently \mathcal{E}_{SN} , is an increasing function of time in the analysed redshift range (Fig. 1 upper panel). The maximum \mathcal{E}_{SN} we can obtain by using the SNR derived from the curve in Fig. 1, a realistic energy transfer efficiency $\epsilon = 0.15$, and $E_{\min} = 10^{-5}$ GeV (Rollinde et al. 2006), is $\mathcal{E}_{\text{SN}}^{\text{max}} \sim 8.6 \times 10^{-28} < 7.4 \times 10^{-27}$ GeV cm $^{-3}$ s $^{-1}$. Note that the ${}^6\text{Li}/\text{H}$ abundance at $z = 3$ results more than one order of magnitude smaller than the value of the simplified case. In the following, we will refer to this physical model as our fiducial model.

We now use the $[\text{Fe}/\text{H}]$ predicted by GAMETE (Fig. 1, lower panel) to convert redshift into $[\text{Fe}/\text{H}]$ values and derive the GM ${}^6\text{Li}$ versus $[\text{Fe}/\text{H}]$. According to our semianalytical model for the build-up of the MW, in fact, the GM elemental abundances reflect those of MPHS, which are predicted to form out of new virialized haloes accreting gas from the GM. This implies that the observed MPHS formed continuously within the redshift range $3 < z \leq 10$. From Fig. 3, we see that our fiducial model yields $\log {}^6\text{Li}/\text{H} = -13.5$, i.e. about three orders of magnitude below the data.

This discrepancy cannot be cured by simply boosting the free parameters to their maximum allowed values. This is also illustrated in the same figure, where for the upper curve we assume $\epsilon = 1$,

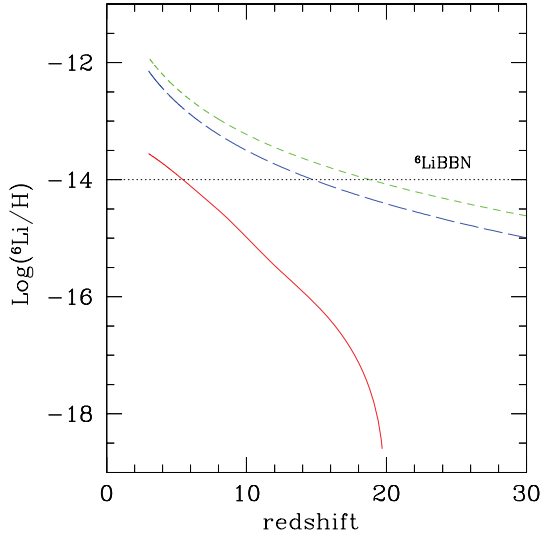


Figure 2. Redshift evolution of GM ${}^6\text{Li}/\text{H}$ abundance for the analytical (green short-dashed line) and numerical solution (overlapped) of a simplified model with no energy losses and destruction, and $\mathcal{E}_{\text{SN}} = 7.4 \times 10^{-27} \text{ GeV cm}^{-3} \text{ s}^{-1}$ for $z > 3$, the same model including energy loss/destruction (blue long dashed line), the fiducial model with realistic SNR, $\epsilon = 0.15$ and $E_{\text{min}} = 10^{-5} \text{ MeV}$ (red solid line).

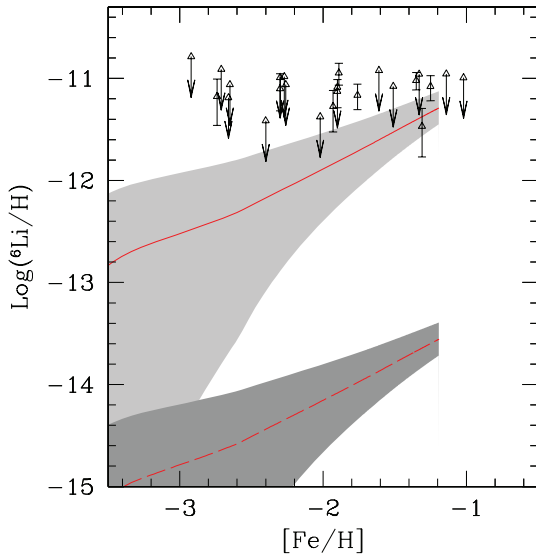


Figure 3. Redshift evolution of ${}^6\text{Li}/\text{H}$ versus $[\text{Fe}/\text{H}]$ for the fiducial model ($\epsilon = 0.15$, $E_{\text{min}} = 10^{-5} \text{ GeV/n}$, dashed line) and for the maximal model ($\epsilon = 1$, $E_{\text{min}} = 10 \text{ MeV/n}$, solid line). The shaded areas denote $\pm 1\sigma$ dispersion regions around the mean.

$E_{\text{min}} = 10 \text{ MeV/n}$ and for the SFR the maximum value allowed by GAMETE within 1σ dispersion. Although the discrepancy between observations and model results is less prominent in this case, we are still unable to fit the data, in particular, at $[\text{Fe}/\text{H}] = -3$ (i.e. at higher redshifts) only $\log {}^6\text{Li}/\text{H} = -12.6$ has had time to be produced, failing short by 30 times.

In addition the flat data distribution cannot be recovered. It is worth noting that, as also pointed out by Asplund et al. (2006), ${}^6\text{Li}$ may be depleted in stars, mainly during the pre-main-sequence phase. If this is the case, the ${}^6\text{Li}$ abundance observed in stars would not be representative of the gas from which they have formed.

Taking into account this effect, the inferred ${}^6\text{Li}$ abundances become metallicity dependent, i.e. the flatness is lost. Because of depletion, however, the derived ${}^6\text{Li}$ values would be higher for all $[\text{Fe}/\text{H}]$, making the discrepancy between our results and observations even larger.

We finally note, as already claimed by Rollinde et al. (2006), that the production of ${}^7\text{Li}$ through this mechanism is comparable with that of ${}^6\text{Li}$, being the production cross-sections of the two isotopes very similar. No overproduction of ${}^7\text{Li}$ is then expected with respect to the BBN-based value.

5 DISCUSSION

We have pointed out that both the level and flatness of the ${}^6\text{Li}$ distribution cannot be explained by CR spallation if these particles have been accelerated by SN shocks inside MW building blocks. Although previous claims (Rollinde et al. 2006) of a possible solution invoking the production of ${}^6\text{Li}$ in an early burst of Pop III stars have been put forward, such a scenario is at odd with both the global properties of the MW and its halo MPHS.

Our model, which follows in detail the hierarchical build-up of the MW and reproduces correctly the MDF of the MPHS, predicts a monotonic increase in ${}^6\text{Li}$ abundance with time, and hence with $[\text{Fe}/\text{H}]$. Moreover, our fiducial model falls short of three orders of magnitude in explaining the data; such discrepancy cannot be cured by allowing the free parameters (E_{min} , ϵ) to take their maximum (physically unlikely) values. Apparently, a flat ${}^6\text{Li}$ distribution appears inconsistent with any (realistic) model for which CR acceleration energy is tapped from SNe: if so, ${}^6\text{Li}$ is continuously produced and destruction mechanisms are too inefficient to prevent its abundance to steadily increase along with $[\text{Fe}/\text{H}]$.

Clearly, the actual picture could be more complex: for example, if the diffusion coefficient in the ISM of the progenitor galaxies is small enough, ${}^6\text{Li}$ could be produced *in situ* rather than in the more rarefied GM. This process might increase the species abundance, but cannot achieve the required decoupling of ${}^6\text{Li}$ evolution from the enrichment history.

Alternatively, shocks associated with structure formation might provide an alternative ${}^6\text{Li}$ production channel (Suzuki & Inoue 2002); although potentially interesting as this mechanism decouples metal enrichment (governed by SNe) and CR acceleration (due to structure formation shocks), the difficulties that this scenario must face are that (i) at the redshifts ($z = 2-3$) at which shocks are most efficient it must be still $[\text{Fe}/\text{H}] < -3$, and (ii) MPHS that formed at earlier epochs should have vanishing ${}^6\text{Li}$ abundance (Prantzos 2006).

If these issues could represent insurmountable problems, then one has to resort to more exotic models involving either suitable modifications of BBN or some yet unknown production mechanism unrelated to cosmic SF history.

ACKNOWLEDGMENTS

We thank M. Kusakabe and E. Rollinde for useful discussions. We thank the referee, M. Asplund, for a careful reading and positive comments.

REFERENCES

- Asplund M., Lambert D. L., Nissen P. E., Primas F., Smith V. V., 2006, *ApJ*, 644, 229
- Blandford R., Eichler D., 1987, *Phys. Rep.*, 154, 1
- Bonifacio P. et al., 2007, *A&A*, 462, 851
- Bromm V., Ferrara A., Coppi P. S., Larson R. B., 2001, *MNRAS*, 328, 969
- Coc A., Vangioni-Flam E., Descouvemont P., Adahchour A., Angulo C., 2004, *ApJ*, 600, 544
- Cole S., Lacey C. G., Baugh C. M., Frenk C. S., 2000, *MNRAS*, 319, 168
- Cumberbatch D., Ichikawa K., Kawasaki M., Kohri K., Silk J., Starkman G. D., 2007, *Phys. Rev. D*, 76, 123005
- Cuoco A., Iocco F., Mangano G., Miele G., Pisanti O., Serpico P. D., 2004, *Int. J. Mod. Phys. A*, 19, 4431
- Cyburt R. H., 2004, *Phys. Rev. D*, 70, 023505
- Daigne F., Olive K. A., Silk J., Stoehr F., Vangioni E., 2006, *ApJ*, 647, 773
- Ganguly R., Sembach K. R., Tripp T. M., Savage B. D., 2005, *ApJS*, 157, 251
- Heger A., Woosley S. E., 2002, *ApJ*, 567, 532
- Heinbach U., Simon M., 1995, *ApJ*, 441, 209
- Hopkins A. M., 2004, *ApJ*, 615, 209
- Jedamzik K., Choi K.-Y., Roszkowski L., Ruiz de Austri R., 2006, *JCAP*, 7, 7
- Jubelgas M., Springel V., Ensslin T., Pfrommer C., 2008, *A&A*, 481, 33
- Kawasaki M., Kohri K., Moroi T., 2005, *Phys. Rev. D*, 71, 083502
- Keshet U., Waxman E., Loeb A., Springel V., Hernquist L., 2003, *ApJ*, 585, 128
- Korn A. J., Grundahl F., Richard O., Barklem P. S., Mashonkina L., Collet R., Piskunov N., Gustafsson B., 2006, *Nat*, 442, 657
- Kusakabe M., Kajino T., Boyd R. N., Yoshida T., Mathews G. J., 2007, *Phys. Rev. D*, 76, 121302
- Lagage P. O., Cesarsky C. J., 1983, *A&A*, 125, 249
- Meneguzzi M., Audouze J., Reeves H., 1971, *A&A*, 15, 337
- Mercer D. J. et al., 2001, *Phys. Rev. C*, 63, 065805
- Miniati F., Ryu D., Kang H., Jones T. W., Cen R., Ostriker J. P., 2000, *ApJ*, 542, 608
- Montmerle T., 1977, *ApJ*, 216, 177
- Omukai K., Tsuribe T., Schneider R., Ferrara A., 2005, *ApJ*, 626, 627
- Pinsonneault M. H., Steigman G., Walker T. P., Narayanan V. K., 2002, *ApJ*, 574, 398
- Pospelov M., 2007, *Phys. Rev. Lett.*, 98, 231301
- Prantzos N., 2006, *A&A*, 448, 665
- Press W. H., 2002, in William H. Press, ed., *Numerical Recipes in C++: The Art of Scientific Computing*, xxviii, 1, 002 p., ill., 26 cm (Includes bibliographical references and index. ISBN: 0521750334)
- Press W. H., Schechter P., 1974, *ApJ*, 187, 425
- Rollinde E., Vangioni E., Olive K., 2005, *ApJ*, 627, 666
- Rollinde E., Vangioni E., Olive K. A., 2006, *ApJ*, 651, 658
- Ryan S. G., Norris J. E., Beers T. C., 1999, *ApJ*, 523, 654
- Salvadori S., Schneider R., Ferrara A., 2007, *MNRAS*, 381, 647
- Salvadori S., Ferrara A., Schneider R., 2008, *MNRAS*, 386, 348
- Schneider R., Ferrara A., Natrajan P., Omukai K., 2002, *ApJ*, 571, 30
- Schneider R., Ferrara A., Salvaterra R., Omukai K., Bromm V., 2003, *Nat*, 422, 869
- Schneider R., Omukai K., Inoue A. K., Ferrara A., 2006, *MNRAS*, 369, 1437
- Spergel D. N. et al., 2007, *ApJS*, 170, 377
- Spite F., Spite M., 1982, *A&A*, 115, 357
- Spite M., Spite F., Maillard J. P., 1984, *A&A*, 141, 56
- Strong A. W., Moskalenko I. V., 1998, *ApJ*, 509, 212
- Suzuki T. K., Inoue S., 2002, *ApJ*, 573, 168
- Tatischeff V., 2008, preprint (arXiv:0804.1004)
- Tatischeff V., Thibaud J.-P., 2007, *A&A*, 469, 265
- Tornatore L., Ferrara A., Schneider R., 2007, *MNRAS*, 382, 945
- Volonteri M., Haardt F., Madau P., 2003, *ApJ*, 582, 559
- Yao W.-M. et al., 2006, *J. Phys. G: Nucl. Phys.*, 33, 1
- Zhao D. H., Mo H. J., Jing Y. P., Börner G., 2003, *MNRAS*, 339, 12

This paper has been typeset from a $\text{\TeX}/\text{\LaTeX}$ file prepared by the author.